Events in evolving three-dimensional vector fields

1980 J. Phys. A: Math. Gen. 13 1

(http://iopscience.iop.org/0305-4470/13/1/003)

J. Phys. A: Math. Gen., **13** (1980) 1–14. Printed in Great Britain

Events in evolving three-dimensional vector fields

J F Nye† and A S Thorndike‡

† H H Wills Physics Laboratory, University of Bristol, Bristol BS8 1TL, UK
‡ Polar Science Center, Division of Marine Resources, University of Washington, Washington, USA

Received 22 January 1979, in final form 8 June 1979

Abstract. For a static three-dimensional vector field $\boldsymbol{u} = \boldsymbol{u}(\boldsymbol{x})$ the set of singular points of the vector function forms a smooth two-dimensional surface embedded in the three-dimensional space of $\boldsymbol{x}$. When this surface is mapped into the three-dimensional space of $\boldsymbol{u}$ there results a surface which typically contains sharp creases, and the shape of this surface characterises the structure of the vector field. As the field evolves with time this singular surface will change, and special points in space–time can be identified where the surface changes its shape in a fundamental way. These changes are called events. The possible events are identified and shown pictorially for general vector fields and for the special case of irrotational fields. The pattern of events gives a morphological way of comparing, say, an observed field with a computed field. If the two fields have the same pattern of events their structures are similar and they are evolving in similar ways.

1. Introduction

Now that three-dimensional time-evolving vector fields without symmetry can be computed numerically, as for example in models of the atmosphere or oceans, the problem arises of comparing an observed with a computed field. Besides quantitative comparison at selected points, one may also ask whether the two fields have the same general structural features. To answer such a question we first need a way of characterising the essential morphology of an evolving three-dimensional vector field. That is what this paper tries to do.

An earlier paper (Thorndike *et al* 1978) has shown how the structure of a static two-dimensional vector field can be characterised by the singularities of the vector function. If the field evolves with time, distinct changes in the geometry of the singular set occur at certain points at certain instants. Such changes were called *events*. What kinds of event will occur naturally in a given physical situation without special symmetry depends on what constraints there are, if any; for example, if we are dealing with the velocity field of a fluid, it might be incompressible. The previous paper gave two lists of events in two-dimensional flows evolving with time: those that occur when there are no constraints, and those that occur when the field is irrotational or incompressible. In experimental work it is an advantage to be able to distinguish such naturally occurring events from the higher singularities which can only be forced by imposed symmetry or other conditions. Examples can be seen in the six-roll mill of Berry and Mackley (1977) (see also Poston and Stewart 1978, especially figure 11.28).

0305-4470/80/010001+14$01.00

This paper extends these results for two-dimensional evolving fields to three-dimensional evolving fields. Events occur at specific points when the evolving three-dimensional singular set undergoes a distinct change in geometry. We list the events that will occur naturally in unconstrained and in irrotational fields. The pattern of events in a field constitutes a basic structure. Two fields that have the same pattern of events may be said to be alike, much as two animals of the same species are alike; they have the same structure and are developing in the same way, without being identical in all respects.

2. Fields with no constraints

The discussion to be given applies to any vector field, but to fix ideas it is helpful to think first of a static smoothly varying three-dimensional velocity field $\boldsymbol{u} = (u, v, w)$:

$$u = u(x, y, z), \qquad v = v(x, y, z), \qquad w = w(x, y, z). \tag{1}$$

We consider the mapping

$$\boldsymbol{u} : X \to U$$

where X represents physical space with coordinates (x, y, z) and U represents velocity space with coordinates (u, v, w). Thus, each point in X is mapped into a corresponding image point in U according to the velocity that exists at the point in X. The singularities under discussion are the sets of points where the determinant of the Jacobian matrix $\partial(u, v, w)/\partial(x, y, z)$ is zero. This condition defines a set of singular points in X. It is with the image in U of these points that we are concerned. If there are no constraints on the flow field, the kinds of stable singularities are those of any general mapping from $\boldsymbol{R}^3$ to $\boldsymbol{R}^3$, namely, fold, cusp and swallowtail (Golubitsky and Guillemin 1973, p 191). In the image space U the folds are surfaces; they are sharply creased along lines of cusps, which we shall call *ribs*, and the ribs themselves have cusp points on them which are the swallowtails.

Now let the field change with time (or any other external parameter). The singular figure in U will evolve and we wish to know what events will occur. To examine this write

$$u = u(x, y, z, t), \qquad v = v(x, y, z, t), \qquad w = w(x, y, z, t), \qquad \tau = t. \tag{2}$$

Considered as a mapping from $\boldsymbol{R}^4$ to $\boldsymbol{R}^4$, the point (x, y, z, t) is mapped to its image (u, v, w, τ); τ is simply the time label in the image space. The list of stable singularities (Golubitsky and Guillemin 1973, p 191) in maps from $\boldsymbol{R}^4$ to $\boldsymbol{R}^4$ is: fold (dimension 3), cusp (2), swallowtail (1), butterfly (0), elliptic umbilic (0) and hyperbolic umbilic (0). In the standard forms for the singularities shown in table 1 at least one pair of variables in each case is simply equated (for example, $u_4 = x_4$). Thus the special maps (2) which have $\tau = t$ can have all the singularities in the list. Each of them is a particular arrangement of fold sheets (hypersurfaces of dimension 3) in the four-dimensional image space. The singular set is easier to visualise if we take successive τ = constant slices and think of the resulting time-evolving three-dimensional figure in U. An event will occur whenever the slice τ = constant passes through a singular point in $\boldsymbol{R}^4$, that is, through an elliptic umbilic, hyperbolic umbilic or butterfly point. Thus, taking the elliptic umbilic as an example, at a particular instant we can expect to see three ribs come together, make contact instantaneously, and then separate.

Table 1. Stable singularities of functions from $\boldsymbol{R}^4$ to $\boldsymbol{R}^4$.

	Vector components			
Singularity	u_1	u_2	u_3	u_4
Fold	x_1^2	x_2	x_3	x_4
Cusp	$x_1^3+x_2x_1$	x_2	x_3	x_4
Swallowtail	$x_1^4+x_3x_1^2+x_2x_1$	x_2	x_3	x_4
Butterfly	$x_1^5+x_4x_1^3+x_3x_1^2+x_2x_1$	x_2	x_3	x_4
Elliptic umbilic	$x_1^2-x_2^2+x_3x_1+x_4x_2$	$x_1x_2+x_4x_1-x_3x_2$	x_3	x_4
Hyperbolic umbilic	$x_1^2+x_3x_2$	$x_2^2+x_4x_1$	x_3	x_4

But there is also another kind of event. With the time dimension present there are lines of swallowtails, surfaces of ribs and hypersurfaces of folds, and so events are possible if a τ = constant slice should meet one of these loci tangentially—just as in $\boldsymbol{R}^3$ a slice tangential to a rib gives a beak-to-beak or lips event. We shall find that tangencies of this kind in $\boldsymbol{R}^4$ can cause two swallowtail points in $\boldsymbol{R}^3$ to come together and annihilate, or, reversing time, for a pair to be created and separate. Moreover, there are three distinct ways in which this encounter between swallowtail points can happen. In a similar way a tangency in $\boldsymbol{R}^4$ of a τ = constant slice with a rib surface produces three distinct kinds of event involving the interaction of ribs in $\boldsymbol{R}^3$.

The orientation of the singular figures in $\boldsymbol{R}^4$ is not completely arbitrary. Since τ plays a special role in the mapping (2) this is not surprising. The consequence is that certain directions of slicing the figures by τ = constant are not allowed, and this limits the types of event that can occur.

These descriptions can now be made more precise. To construct a time-dependent vector field of the form (2) having one of the singularities in table 1, one can make any smooth reversible transformation

$$(x_1, x_2, x_3, x_4) \to (x, y, z, t),$$

$$(u_1, u_2, u_3, u_4) \to (u, v, w, \tau),$$

which results in $\tau = t$. In the cuspoids, the first four in the table, this precludes putting $\tau = u_1$. In the two umbilics it precludes both $\tau = u_1$ and $\tau = u_2$. These prohibitions embody the restriction referred to above on the orientation of the singular set in the image space. (If we consider the fold with two space dimensions and one time dimension, the fact that τ cannot be identified with u_1 means that the fold surface cannot be tangential to the observation plane τ = constant at any point. This restriction affects higher singularities. For example, $\tau = u_1$ for the swallowtail would orient the swallowtail figure in the image space so that, approaching the origin, folds would become parallel to τ = constant, and this is forbidden.)

Table 2 gives examples, constructed by using these principles, of the possible events. To illustrate the construction, the first entry in table 2 can be produced from the standard form of the cusp in table 1 by a change of coordinates of the form

$$(x_1, x_2, x_3, x_4) = (x, t+y^2+z^2, y, z),$$

$$(u_1, u_2, u_3, u_4) = (u, \tau+v^2+w^2, v, w).$$

(Numerical coefficients must be inserted in this change of coordinates to produce the

Table 2. Examples of events in unconstrained vector fields.

Event		Vector field u	v	w
Cusp events	(1) Elliptic rib collapse (lips)	$-4x^3-2(t+y^2+z^2)x$	y	z
	(2) Elliptic rib collapse (beak-to-beak)	$-4x^3+2(t+y^2+z^2)x$	y	z
	(3) Hyperbolic rib interchange (lips and beak-to-beak)	$-4x^3-2(t-y^2+z^2)x$	y	z
Swallowtail pairs	Head-to-head	$-5x^4-3(t-z^2)x^2-2yx$	y	z
	Tail-to-tail	$-5x^4+3(t-z^2)x^2-2yx$	y	z
	Side-to-side	$-5x^4-3yx^2-2(t-z^2)x$	y	z
Elliptic umbilic		$-3x^2+3y^2-2tx-2zy$	$6xy$ $-2ty+2zx$	z
Hyperbolic umbilic		$-3x^2-zy$	$-3y^2-tx$	z
Butterfly	τ with u_4	$-6x^5-4tx^3-3zx^2-2yx$	y	z
	τ with u_3	$-6x^5-4yx^3-3tx^2-2zx$	y	z
	τ with u_2	$-6x^5-4yx^3-3zx^2-2tx$	y	z

forms given in table 2. The choices of coefficients there were made to simplify the forms in table 3.)

The different ways in which a rib surface can be met tangentially by τ = constant result in three distinct rib interactions which can be pictured as time-evolving figures in $\boldsymbol{R}^3$. (1) Elliptic (figure 1): a pie-shaped figure in which the two surfaces are folds and the edge is a rib. This collapses to a point and vanishes. It is a lips event rotated in three dimensions. (2) Elliptic (figure 2): this is a beak-to-beak event rotated in three dimensions. It has the same rib configuration as (1) but with the fold surfaces outside the rib instead of inside. Two fold surfaces join on a circular (elliptical) rib, the inside of the circle being empty. As time evolves the circle collapses and the two fold surfaces separate. (3) Hyperbolic (figure 3): two ribs form the branches of a hyperbola. As time

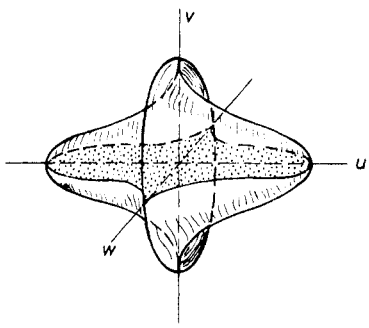

Figure 1. Elliptic rib collapse (1). The event occurs as this surface in (u, v, w) shrinks to a point and vanishes. In this and the other three-dimensional sketches which follow, the bold line is a rib, here an ellipse in the $u = 0$ plane.

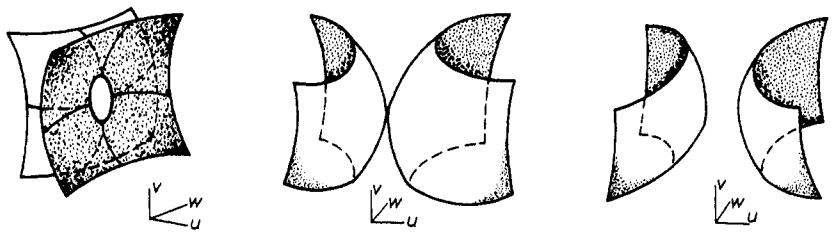

Figure 2. Elliptic rib collapse (2). The sequence of sketches reading from left to right shows the singular set before, at, and after the event. The event can be reversed by changing the sign of t in table 2.

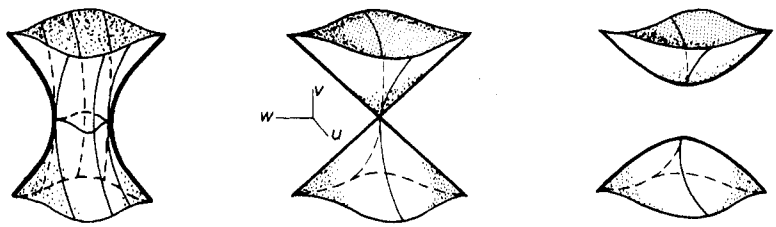

Figure 3. Hyperbolic rib interchange.

evolves they become the asymptotes of the hyperbola (this is the event), and then they separate into the other two sectors between the asymptotes. One principal section shows lips, while the other shows beak-to-beak. In each of these events, and in the others which follow, time can be reversed.

A pair of swallowtails can meet in three ways, head-to-head (figure 4), tail-to-tail (figure 5) or side-to-side (figure 6), depending on how τ is allocated.

In both the elliptic umbilic (figure 7) and the hyperbolic umbilic the possible allocations of τ and t provide only one type of event. The hyperbolic umbilic event is sketched in figure 11(a) of Thorndike *et al* (1978). The event occurs as the swallowtail points S_1 and S_2 move together, meet, and then separate. In this case the swallowtails are side-to-side but antiparallel.

In the butterfly τ can be allocated to u_2, u_3 or u_4 but not u_1. The way in which τ is allocated determines the orientation of the singular set in (u, v, w, τ) space. Therefore,

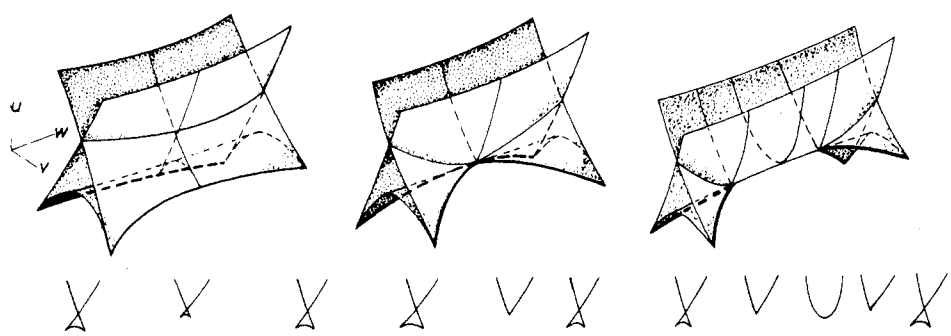

Figure 4. Swallowtail pair, head-to-head.

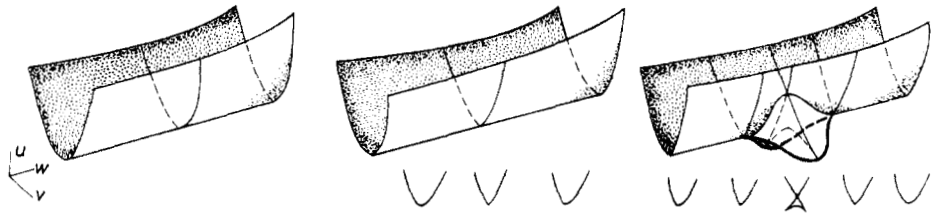

Figure 5. Swallowtail pair, tail-to-tail.

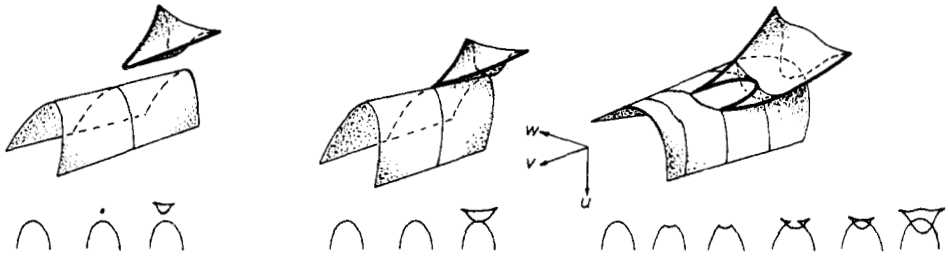

Figure 6. Swallowtail pair, side-to-side.

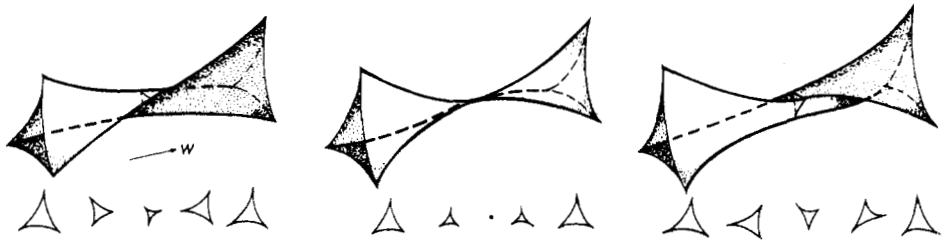

Figure 7. Elliptic umbilic.

the sequence of three-dimensional singular sets we see by taking successive slices τ = constant will depend on how τ is allocated. We have chosen to display the butterfly in the form of a two-dimensional array of two-dimensional computed pictures (figure 8). In this form two of the four control variables are the (outside) coordinates for the array and the remaining two are the (inside) coordinates for each 'postage stamp.' There are six ways to choose two objects from four and we present all six. Even though each of the six diagrams gives a complete picture of the same object in $\boldsymbol{R}^4$, there are remarkable differences in appearance. One should keep in mind that, because these sections by the coordinate planes have special symmetry, some unsymmetrical features of a more general section may be lost (see the swallowtail example in figure 7 of Thorndike *et al* (1978)). The sequence of three-dimensional sketches of the butterfly given in Thom (1975, pp 70–71) shows the time-evolving figure for the first of the three forms given in table 2.

We believe that the list of events in table 2 is exhaustive but we have no formal proof. However, the examples given show that the events listed can indeed exist. When thought of as mappings from $\boldsymbol{R}^4$ to $\boldsymbol{R}^4$, each entry in table 2 is equivalent to one in table 1, but we regard them as distinct events because of the different ways the singular sets are oriented with respect to the slices τ = constant. Our intuitive approach meets a

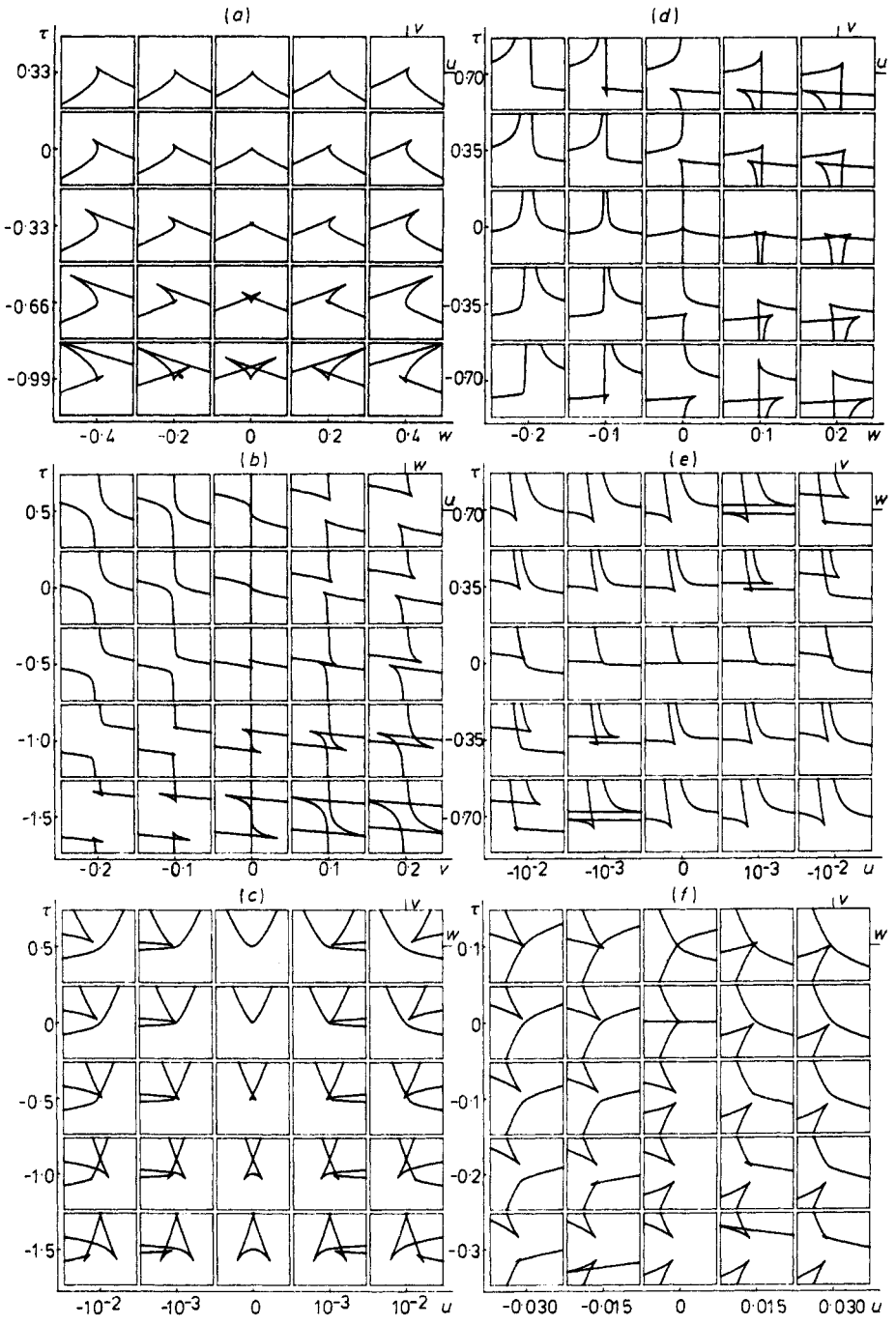

Figure 8. Butterfly. Diagrams (*a*), (*b*), and (*c*) are computed from the first butterfly form in table 2; (*d*) and (*e*) refer to the second form; (*f*) refers to the third form. For the second form no diagram is given with τ, v as the outside coordinates, since it would simply be the transpose of the τ, w diagram for the first form—diagram (*a*). Similarly, the τ, v and τ, w diagrams for the third form are redundant with diagrams (*b*) and (*d*). Each diagram represents the same object in (u_1, u_2, u_3, u_4) space; thus diagram (*a*) corresponds to outside coordinates u_4, u_3; (*b*) $\rightarrow u_4, u_2$; (*c*) $\rightarrow u_4, u_1$; (*d*) $\rightarrow u_3, u_2$;(*e*) $\rightarrow u_3, u_1$; (*f*) $\rightarrow u_2, u_1$. The locus of swallowtails can be picked out in each diagram.

formal difficulty here which we have not solved, namely the stability of these events as one-parameter families of mappings $\boldsymbol{R}^3 \to \boldsymbol{R}^3$. This problem needs a more rigorous treatment.

3. Irrotational fields

We turn now to an example of a field subject to a constraint, namely a vector field that is irrotational. This case is chosen both for its physical importance (gravitational, electric and heat-flow fields come to mind as examples) and because the list of events can be deduced from catastrophe theory. We start with any one of the standard generating functions from catastrophe theory (we would call it a family of potentials but we need the word potential for another purpose) $\Phi(x, y, z, t; u, v, w, \tau)$, where x, y, z, t are state variables and u, v, w, τ are controls. These functions are listed in Poston and Stewart (1978, p 121). If Φ can be written in the form

$$\Phi(x, y, z, t; u, v, w, \tau) = \phi(x, y, z, \tau) + ux + vy + wz - \tfrac{1}{2}t^2 + \tau t \tag{3}$$

(and we shall show that it can be so written), the stationary condition

$$\Phi_x = \Phi_y = \Phi_z = \Phi_t = 0, \tag{4}$$

where subscripts denote differentiation, implies

$$u = -\phi_x, \qquad v = -\phi_y, \qquad w = -\phi_z, \qquad \tau = t,$$

which describes an irrotational time-dependent vector field derived from the scalar potential $\phi(x, y, z, \tau)$. The singularities of the gradient mapping (4) (coalescences of the critical points of Φ) are Thom's (1975) list of catastrophes of codimension up to four: fold, cusp, swallowtail and butterfly, together with the elliptic, hyperbolic and parabolic umbilics. Each of these corresponds to a singular set in control space (u, v, w, τ) and it is this four-dimensional figure that we have to slice with $\tau =$ constant.

At any instant the singular set in (u, v, w) can be fold, cusp, swallowtail, or elliptic or hyperbolic umbilic. In (u, v, w, τ) the parabolic umbilic and butterfly are points, the elliptic and hyperbolic umbilic and swallowtail are lines (the tracks of moving points), the ribs are surfaces (the tracks of moving lines), and the folds are hypersurfaces (dimension 3). Thus the possible events are parabolic umbilic and butterfly (as the $\tau =$ constant slice passes through one of these points), together with events arising from tangencies between $\tau =$ constant and one of the above loci. These latter, as we shall show by example, give two new pair creation or annihilation events not found in unconstrained fields, namely pairs of elliptic and pairs of hyperbolic umbilics. This means that in (u, v, w) at, say, $\tau < 0$ there are two elliptic or two hyperbolic point singularities; they move together to meet at $\tau = 0$ and then disappear. We also have swallowtail pairs, as before, and the cusp events described previously.

Table 3 shows examples of these events by listing time-dependent potentials $\phi(x, y, z, \tau)$ which give them. To obtain the examples we start with standard forms (Poston and Stewart 1978, p 121) for $\Phi(X, Y, Z, T; a, b, c, d)$ where X, Y, Z, T are state variables and a, b, c, d are controls, and make smooth reversible changes of coordinates: first $(X, Y, Z, T) \to (x, y, z, t)$ where a, b, c, d may appear as parameters, and then $(a, b, c, d) \to (u, v, w, \tau)$ to bring Φ into the form (3), an essential feature of (3) being that x, y, z appear linearly in the terms ux, vy, wz.

Table 3. Examples of events in irrotational vector fields.

Event		Flow potential $\phi(x, y, z, \tau)$
Cusp events	(1) Elliptic rib collapse (lips)	$x^4+(\tau+y^2+z^2)x^2-\frac{1}{2}y^2-\frac{1}{2}z^2$
	(2) Elliptic rib collapse (beak-to-beak)	$x^4-(\tau+y^2+z^2)x^2-\frac{1}{2}y^2-\frac{1}{2}z^2$
	(3) Hyperbolic rib interchange (lips and beak-to-beak)	$x^4+(\tau-y^2+z^2)x^2-\frac{1}{2}y^2-\frac{1}{2}z^2$
Swallowtail pairs	Head-to-head	$x^5-\frac{1}{2}x^4+(\tau-z^2)x^3+yx^2-\frac{1}{2}y^2-\frac{1}{2}z^2$
	Tail-to-tail	$x^5-\frac{1}{2}x^4-(\tau-z^2)x^3+yx^2-\frac{1}{2}y^2-\frac{1}{2}z^2$
	Side-to-side	$-\frac{1}{2}x^6+x^5+yx^3+(\tau-z^2)x^2-\frac{1}{2}y^2-\frac{1}{2}z^2$
Elliptic umbilic pair		$x^3-3xy^2+(\tau-z^2)(x^2+y^2)-\frac{1}{2}z^2$
Hyperbolic umbilic pair		$x^3+y^3+(\tau-z^2)xy-\frac{1}{2}z^2$
Butterfly	τ with x^4	$\frac{1}{2}x^6+(\tau-\frac{1}{2})x^4+zx^3+yx^2-\frac{1}{2}y^2-\frac{1}{2}z^2$
	τ with x^3	$-\frac{1}{2}x^8+x^6+(y-\frac{1}{2})x^4+\tau x^3+zx^2-\frac{1}{2}y^2-\frac{1}{2}z^2$
	τ with x^2	$-\frac{1}{2}x^8+\frac{1}{2}x^6+yx^4+zx^3+\tau x^2-\frac{1}{2}y^2-\frac{1}{2}z^2$
Parabolic umbilic	τ with x^2	$x^2y+\frac{1}{2}y^4+\tau x^2+zy^2-\frac{1}{2}z^2$
	τ with y^2	$-\frac{1}{2}x^4+x^2y+y^4+zx^2+\tau y^2-\frac{1}{2}z^2$

For the cusp events the standard form

$$X^4+aX^2+bX-\tfrac{1}{2}Y^2-\tfrac{1}{2}Z^2-\tfrac{1}{2}T^2$$

with the coordinate changes

$$(X, Y, Z, T)=(x, y-c, z-d, t-a), \qquad (a, b, c, d)=(\tau, u, v, w),$$

gives

$$\phi=x^4+\tau x^2-\tfrac{1}{2}y^2-\tfrac{1}{2}z^2.$$

Terms involving only control variables have been dropped since they do not affect the stationary condition (4). The three forms in table 3 result from replacing τ in ϕ by $\tau+y^2+z^2$, $-\tau-y^2-z^2$, $\tau-y^2+z^2$, thereby adding terms in y^2x^2 and z^2x^2. These terms make no essential difference to the cusp nature of the singularity, but they have the effect of bending its locus $u=0$, $\tau=0$ so that it is no longer a plane but becomes instead a curved surface tangent to $\tau=0$ at the origin.

For the swallowtail pairs the standard form

$$X^5+aX^3+bX^2+cX-\tfrac{1}{2}Y^2-\tfrac{1}{2}Z^2-\tfrac{1}{2}T^2$$

with coordinate changes (of a type we learned from Dr David Rand)

$$(X, Y, Z, T)=(x, y-x^2-b, z-d, t\mp a), \qquad (a, b, c, d)=(\pm\tau, v, u, w),$$

$$(X, Y, Z, T)=(x, y-x^3-a, z-d, t-b), \qquad (a, b, c, d)=(v, \tau, u, w),$$

gives, respectively,

$$\phi = x^5 - \tfrac{1}{2}x^4 \pm \tau x^3 + yx^2 - \tfrac{1}{2}y^2 - \tfrac{1}{2}z^2$$

and

$$\phi = -\tfrac{1}{2}x^6 + x^5 + yx^3 + \tau x^2 - \tfrac{1}{2}y^2 - \tfrac{1}{2}z^2.$$

The forms in table 3 are obtained by replacing τ by $\tau - z^2$, thus bending the swallowtail locus so that it has a point of tangency with $\tau = 0$. The singular sets for the first six events in table 3 have been plotted and observed to have the same local structures as those in figures 1–6. (An identical procedure was used on page 1471 of the earlier paper to produce examples of the swallowtail in two space dimensions and one time dimension. Note that a term in x^5 was neglected in error there.)

As shown in the earlier paper, the elliptic and hyperbolic umbilics are stable points in evolving two-dimensional irrotational fields. With one more space dimension the locus of these points is a line. Just as with the swallowtail we have inserted $\tau - z^2$ in the forms in table 3 for these events to bend this line so that it meets $\tau = 0$ tangentially. The pair events which result are illustrated in figures 9 and 10.

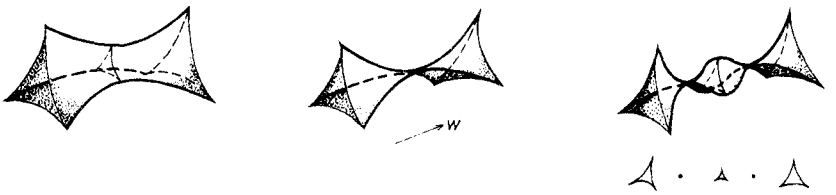

Figure 9. Elliptic umbilic pair.

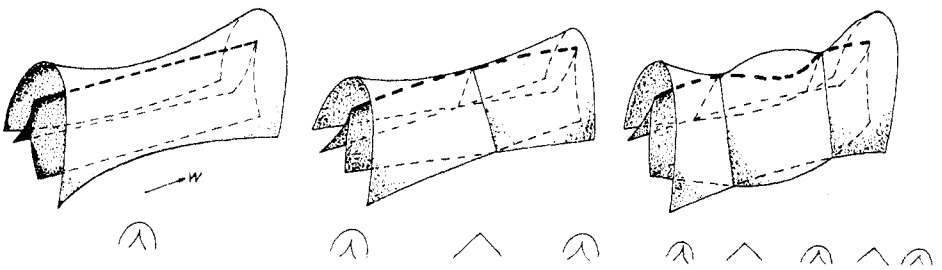

Figure 10. Hyperbolic umbilic pair.

For the butterfly events, the entries in table 3 were produced from the standard form

$$X^6 + aX^4 + bX^3 + cX^2 + dX - \tfrac{1}{2}Y^2 - \tfrac{1}{2}Z^2 - \tfrac{1}{2}T^2$$

by the coordinate changes

$$(X, Y, Z, T) = (x, y - x^2 - c, z - x^3 - b, t - a), \qquad (a, b, c, d) = (\tau, w, v, u),$$

$$(X, Y, Z, T) = (x, y - x^4 - a, z - x^2 - c, t - b), \qquad (a, b, c, d) = (v, \tau, w, u),$$

$$(X, Y, Z, T) = (x, y - x^4 - a, z - x^3 - b, t - c), \qquad (a, b. c. d) = (v, w, \tau, u).$$

The velocity fields given by these potentials may be obtained from the corresponding fields in table 2 by coordinate changes in X which are smooth and non-singular everywhere; for example, to obtain the first field put $(x, y, z) = (x', y' - x'^2, z' - x'^3)$. Since no coordinate change is needed in U, the evolving singular set in U (as shown in figure 8) is exactly the same whether it is calculated with the field of table 2 or the corresponding irrotational field of table 3.

Similarly, the entries for the parabolic umbilic were obtained from the standard form

$$X^2Y + Y^4 + aX^2 + bY^2 + cX + dY - \tfrac{1}{2}Z^2 - \tfrac{1}{2}T^2$$

by the coordinate changes

$$(X, Y, Z, T) = (x, y, z - y^2 - b, t - a), \qquad (a, b, c, d) = (\tau, w, u, v),$$

$$(X, Y, Z, T) = (x, y, z - x^2 - a, t - b), \qquad (a, b, c, d) = (w, \tau, u, v).$$

Computed sections of the parabolic umbilic are shown in figure 11, and from these sections the two corresponding time-evolving figures in U have been sketched in figure 12. The second form is quite special in that the section $\tau = 0$ contains the complete locus of beak-to-beak and lips; thus at $\tau = 0$ an entire line of lips and beak-to-beak appears momentarily. Further details of the parabolic umbilic singularity are given by Godwin (1971).

4. Discussion

We have listed the events that will occur naturally in three-dimensional vector fields as they evolve with time when the field is either unconstrained or irrotational. For the necessary proof of the stability of the singular sets in $\boldsymbol{R}^4$ we have relied on the list established by others for the stable singularities in maps from $\boldsymbol{R}^4$ to $\boldsymbol{R}^4$, and on Thom's list of the elementary catastrophes. Our two lists of possible events have been obtained by considering what ways there are of slicing the singular sets by holding time constant. The purpose of the examples in tables 2 and 3 is to establish the existence of the events listed. There may be other kinds of events, but we believe not. The sections illustrated in the figures for the butterfly and parabolic umbilic, although numerous, are not, of course, exhaustive, but we hope they will serve as a guide to what one may expect to see in experiments.

Our lists of events differ from that given by Wassermann (1975, p 105) for 'time-stable' unfoldings, but this is not unexpected because Wassermann approaches what appears to be an essentially different problem. His problem is set firmly in the context of catastrophe theory. To give a tentative example, suppose there is a three-dimensional inhomogeneous body (a cloud of interstellar gas perhaps) which has a distribution of density $\rho(x, y, z, t)$, and suppose the physics is such that the actual (equilibrium) density at (x, y, z, t) is obtained by minimising some smooth potential $\Phi(\rho; x, y, z, t)$ with respect to ρ. Thus ρ is the state variable and x, y, z, t are controls. Distinguishing t from x, y, z, Wassermann lists the singular sets in control space which correspond to degenerate critical points of Φ.

Note particularly that there is no function from ρ to (x, y, z, t)—a given ρ will be found at many points in space–time—and that the singular sets considered occur in space–time. Our problem is different, not only because x, y, z, t are state variables

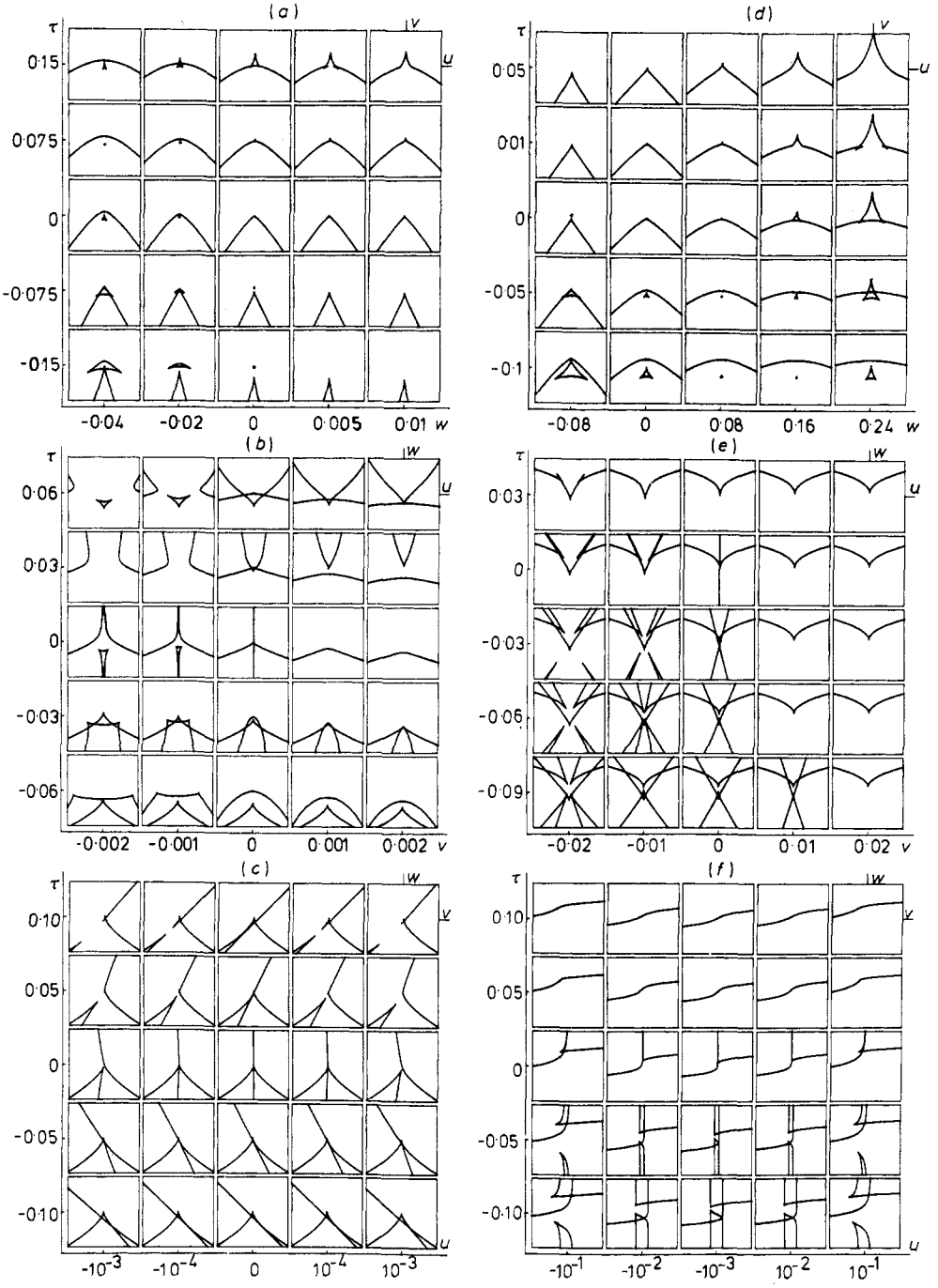

Figure 11. Parabolic umbilic. Diagrams (*a*), (*b*) and (*c*) are computed from the first form for the parabolic umbilic in table 3; (*d*), (*e*), and (*f*) refer to the second form. As for the butterfly in figure 8, the six diagrams all represent the same object in $\boldsymbol{R}^4$: diagram (*a*) corresponds to outside coordinates *a*, *b*; (*b*) → *a*, *d*; (*c*) → *a*, *c*; (*d*) → *b*, *a*; (*e*) → *b*, *d*; (*f*) → *b*, *c*. Thus (*a*) and (*d*) are essentially the same. The remaining section with outside coordinates *c*, *d* is missing because τ, which is always chosen to be an outside coordinate, is never associated with either *c* or *d*.

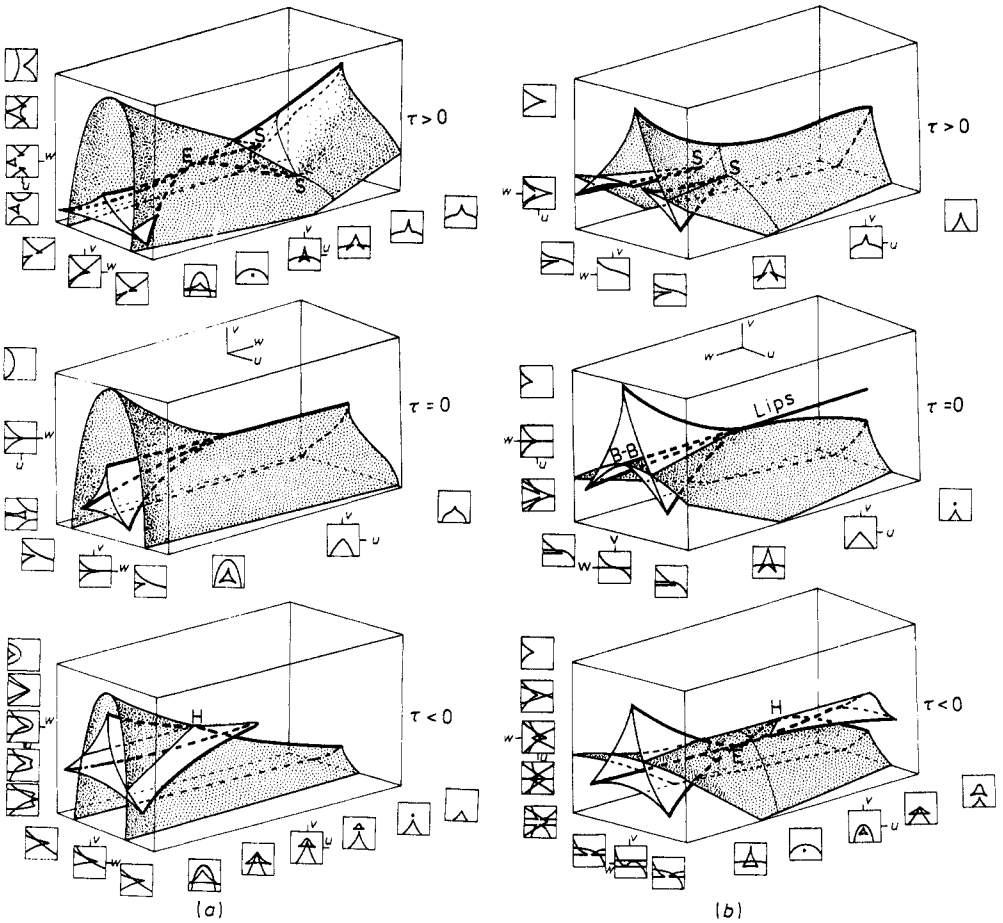

Figure 12. Parabolic umbilic. (*a*) corresponds to the first form in table 3 and to (*a*), (*b*) and (*c*) of figure 11. (*b*) corresponds to the second form of table 3 and to (*d*), (*e*) and (*f*) of figure 11. E, elliptic umbilic; H, hyperbolic umbilic; S, swallowtail; B-B, beak-to-beak.

rather than controls, but because we have a function from state space to control space: each (x, y, z, t) determines a unique (u, v, w, τ) (this was ensured by the form (3)). Thus, there seems no reason why the lists of events should be the same.

With only two space dimensions it was possible, by using a generating function, to treat flows that are either irrotational or incompressible. Rather naturally one can also treat two-dimensional flows that are simultaneously irrotational and incompressible (so that the potential obeys Laplace's equation). In that case the stable singularities in $\boldsymbol{R}^2$ at given time are merely points (see the Appendix), degenerate remnants of the folds and cusps which appear under lighter constraints. In the optical analogy (Thorndike *et al* 1978, p 1478) the points are simply elliptic umbilic foci at infinity. When the field is allowed to change with time, the singular points move around in the image space but do not collide.

This may be an instance of a general rule. For time-dependent two-dimensional flows no constraints give three different kinds of event. The constraint of being either irrotational or incompressible increases the number to five. But when both constraints

are imposed at once the number falls to zero. Richness of behaviour can depend, as in other contexts, on some restriction but not too much.

With three space dimensions we have not found a way of treating incompressible flow. What kind of events will occur naturally in a time-evolving three-dimensional incompressible flow is not known; it is a problem that deserves further study.

Acknowledgments

We are grateful for support for this work from the National Science Foundation Grant DPP7720885 to the University of Washington.

Appendix. Singular points in a two-dimensional flow that is both irrotational and incompressible

With potential $\phi(x, y)$ an irrotational flow field is $u = -\phi_x$, $v = -\phi_y$, and a point is singular if the Jacobian $\partial(u, v)/\partial(x, y) \equiv \phi_{xx}\phi_{yy} - \phi_{xy}^2 = 0$. This equation defines a line (fold-line) in (x, y). But, if the flow is also incompressible, $\phi_{xx} + \phi_{yy} = 0$ and a point is singular if $-\phi_{xx}^2 - \phi_{xy}^2 = 0$. This implies the two equations $\phi_{xx} = \phi_{xy} = 0$, which define isolated points in (x, y).

To see that the points do not collide, first note that, since it obeys Laplace's equation, ϕ can be expressed as the real part of any analytic function f of a complex variable $\zeta = x + iy$. The condition for a singular point is then $f''(\zeta) = 0$. The roots of this equation are isolated points in the complex plane. With time the points will move in the plane; at special times the real parts of two roots will be equal and at others the imaginary parts will be equal, but typically not both at the same time. So the points will not collide unless a further constraint is applied.

References

Berry M V and Mackley M R 1977 *Phil. Trans. R. Soc.* A **287** 1–16
Godwin A N 1971 *Inst. Hautes Etudes Sci. Publ. Math.* **40** 117–38
Golubitsky M and Guillemin V 1973 *Stable Mappings and their Singularities* (New York: Springer)
Poston T and Stewart I N 1978 *Catastrophe Theory and its Applications* (London: Pitman)
Thom R 1975 *Structural Stability and Morphogenesis* (Reading, Mass: Benjamin) (translation of *Stabilité Structurelle et Morphogénèse* (1972) (Reading, Mass: Benjamin))
Thorndike A S, Cooley C R and Nye J F 1978 *J. Phys. A: Math. Gen.* **11** 1455–90
Wasserman G 1975 *Acta Math.* **135** 57–128